POLITECNICO DI TORINO
Repository ISTITUZIONALE

Multi-spectral sensors monitoring of the epidemic of Xylella Fastidiosa in the Apulia Region

Original
Multi-spectral sensors monitoring of the epidemic of Xylella Fastidiosa in the Apulia Region / Dell'Anna, S., Mansueto, G., Boccardo, P., Arco, E.. - ELETTRONICO. - (2022), pp. 610-615. (2022 IEEE 21st Mediterranean ...) [10.1109/MELECON53508.2022.9843049].

Availability:
This version is available at: 11583/2985240 since: 2024-01-19T13:54:08Z

Publisher:
IEEE

Published
DOI:10.1109/MELECON53508.2022.9843049

Terms of use:

This article is made available under terms and conditions as specified in the corresponding bibliographic description in the repository

Publisher copyright
ACM postprint/Author's Accepted Manuscript

(Article begins on next page)

18 November 2026

Multi-spectral sensors monitoring of the epidemic of *Xylella Fastidiosa* in the Apulia Region

2022 IEEE 21st Mediterranean Electrotechnical Conference (MELECON) | 978-1-6654-4280-0/22/$31.00 ©2022 IEEE | DOI: 10.1109/MELECON53508.2022.9843049

Sara Dell'Anna
Politecnico di Torino, Corso Duca degli Abruzzi 24
Turin, Italy
saradellanna12@gmail.com

Giuseppe Mansueto
ITHACA, Via Pier Carlo Boggio 61
Turin, Italy
g.mansueto94@gmail.com

Piero Boccardo
DIST, Politecnico di Torino, Viale Mattioli 39
Turin, Italy
piero.boccardo@polito.it

Emere Arco
DIST, Politecnico di Torino, Viale Mattioli 39
Turin, Italy
emere.arco@polito.it

In October 2013, the Apulia Region in Italy, unexpectedly, had to find itself to face the epidemic of Xylella Fastidiosa which in less than 10 years has decimated millions of olive trees, endangering the 40% of the regional olive-growing heritage. Taking into account the fact that there is not a definitive cure discovered yet, the only solution is the prevention linked to constant monitoring in the so-called buffer areas with diligent efforts to delimitate the phenomenon on a very local scale. Back then, remote sensing and, in particular, multispectral and hyperspectral sensors, seemed to be the key to depicting the problem to a multidimensional extent and coming up with the most adequate ways to tackle it. This research work focuses on the analysis of 4 olive groves (of the Ogliarola cultivar) in the province of Brindisi (Italy), with different symptomatic states, using a multispectral sensor mounted on a UAV system. Among a number of different vegetation indexes (IVs) calculated, the GNDVI and the BNDVI outperform to identify the effects of the Xylella Fastidiosa infection, which was further confirmed by the laboratory analyses. This confirmation has affirmed the validity of the approach used aiming at identifying "anomalies" on non-symptomatic trees and establishing a first early warning system for a subsequent more in-depth investigation in the field. Further developments will investigate the implementation of a segmentation algorithm, according to the threshold values of the IVs defined in this work, and the use of hyperspectral sensors, in order to identify anomalies on the foliage, attributable to a potential Xylella Fastidiosa infection on the trees.

Keywords — Xylella Fastidiosa, Olive groves, Multispectral, Early warning

I. INTRODUCTION

The Xylella Fastidiosa (XF) bacterium has destroyed the 40% of the Apulian olive-growing heritage, causing a real epidemic, the so-called Olive Quick Decline Syndrome (OQDS). The disease balance is catastrophic: 8000 km2 of dried olive groves, 1.6 billion of estimated economic loss [1], countless historical and cultural damage. The head of the disease spread at a regional scale is a 10 mm insect, Philaenus spumarius, which transports the infection from an affected tree to a healthy one. In order to reduce the spread, the Region, half-yearly, has imposed phytosanitary treatments which have slowed down the phenomenon. From the monitoring perspective, the only way to keep track of the disease is carried out through field sampling campaigns, followed by laboratory analysis, and through the use of remote sensors. The former is currently the only certificated method able to establish the actual presence of the bacterium in the tree; while the latter, even if it is less time consuming and requires less workforce, is still in an experimental stage.

Previous studies in the context [2] have already been carried out through hyperspectral and thermal sensors, in tune with the needs of the scientific community. The aim of this research is the detection of "anomalies" on the canopy of non-symptomatic trees, establishing a first early warning system for a preliminary screening phase, followed by more in-depth investigations in the field.

II. INSTRUMENT

The input dataset is composed by multispectral images acquired by a multispectral sensor mounted on an unmanned aerial vehicle (UAV). The drone used for this study is the high-precision Phantom 4 Multispectral, endowed with multispectral imaging system mostly addressed to precision farming. The sensor is equipped with 6 cameras: 5 narrowband and an RGB; with each camera possessing an effective resolution of 2.08 Mpx with global shutter and 3-axis stabilization. The FOV (Field of View) is 62.7° and the focal length is 5.74 mm. The UAV system has an integrated light system that catches the irradiation in order to ensure the accuracy and the homogeneity of the acquired data.

The images are georeferenced automatically through the DJI TimeSync system adopted for the high-precise measurements (centimetre-size) [3].

The sensor is endowed with an array of 5 multispectral cameras: tree of which catch the radiance from the visible region of the spectrum (Red, Green, Blue), while the other two acquire the radiation from the so-called infrared zones (which goes from the red edge, which goes from 714 nm to 746 nm) and from NIR (Near-Infrared) (Table 1).

Authorized licensed use limited to: Politecnico di Torino. Downloaded on January 18,2024 at 18:24:35 UTC from IEEE Xplore. Restrictions apply.

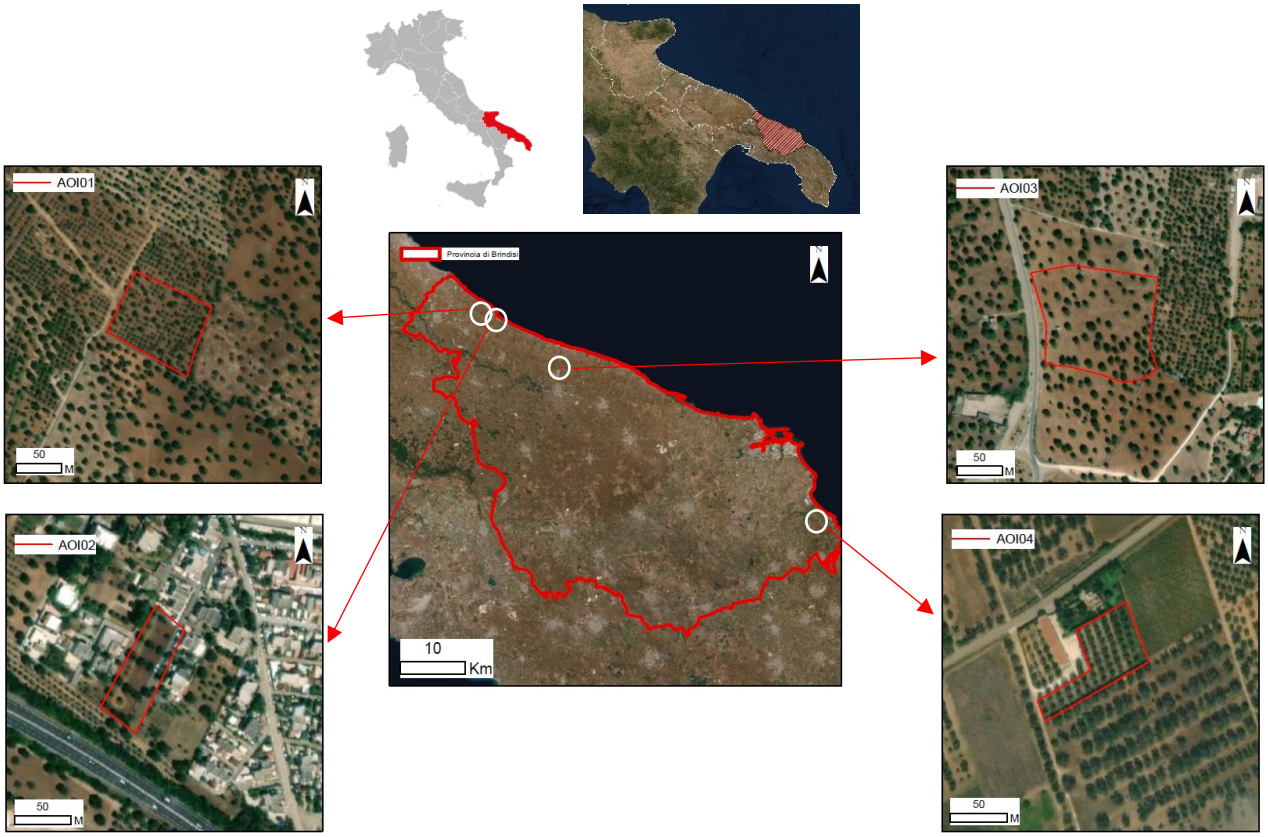


Fig. 1. Areas of Interest (AOI) in Brindisi province. Source: Esri, Maxar, GeoEye, Earthstar Geographics, CNES/Airbus DS, USDA, USGS, AeroGRID, IGN, and the GIS User Community

TABLE 1. ACQUISITION BANDS OF PHANTOM 4 MULTISPECTRAL

	Λ (nm)	Band width (nm)
Blue	450	32
Green	560	32
Red	670	32
Res Edge	730	32
NIR	840	52

The imageries over the four olive groves were acquired by multispectral sensor through aerial survey at 30 and 70 meters Above Ground Level (AGL). Additionally, further imageries at canopy scale (15 meters AGL) were acquired, in order to extract more detailed information about the single branches.

III. CASE STUDY

Even though Lecce, the southernmost province of the Apulia Region, was initially hit by the infection in 2013; the affected olive groves located in this area are still observed to be in almost - dried state.

As the objective of this study is to extract information through the sensors, it is necessary for the cameras to catch the radiance emitted by the leaves on the foliage - which acts as a marker on the status of health of the trees.

In the light of this reasoning, the Brindisi area (Fig. 1) was selected for this case study. It is located almost at 40 km distance in the Northern direction from Lecce. The effects of the XF in Brindisi were, generally, less evident than those observed in Lecce.

The analysis concerned 4 olive groves (Fig.1): three Areas of Interest (AOI) (AOI01, AOI02, AOI03) host centuries-old trees, that belong to Ogliarola cultivar, while in the fourth area (AOI04) younger olive trees (25-30 years old) of the Cellina cultivar are present. The first survey (AOI01, AOI02, AOI03) was performed on October 25th, 2021, while the second survey (AOI04) was on November 3rd, 2021.

The four land parcels have different symptomatic states, as described below:

- AOI01 (Fasano, 7 000 m^2): The olive trees did not show any symptoms.
- AOI02 (Fasano, 3 000 m^2): Only a single olive tree had a tiny damaged segment on the foliage. The rest of the trees did not have any signs of infection or symptoms. The laboratory analyses, carried out by Phytosanitary District of the Apulia Region (published on November 4th, 2021), demonstrated that the trees tested positive to the bacteria presence.

Authorized licensed use limited to: Politecnico di Torino. Downloaded on January 18,2024 at 18:24:35 UTC from IEEE Xplore. Restrictions apply.

- AOI03 (Ostuni, 14 000 m^2): Some of the olive trees were identified with dried branches. Some of the olive trees have been identified with dead branches. However, the percentage of dried foliage on the trees does not affect the survey as these were pruned shortly before.
- AOI04 (San Pietro Vernotico, 3 000 m^2): The olive trees were in advanced infectious state. The majority of the canopy is affected.

IV. METHOD

The values recorded in the bands of the acquired multispectral images were analysed through the use of vegetation indices (VIs). VI are maths combination: ratios between the reflectance values associated with the different bands of the spectrum [4]. The mathematical expressions are formulated in such a way to minimize the interference due to the survey (e.g. images geometrical distortion, sensors radiometric instability, atmospheric and topographic effect) [5] and highlight specific stress, enabling the remote control of the plant health and its needs, in terms of water, nutrients and fertilizers.

The acquired imageries were processed using 3 different software: DJI Terra, Pix4D. Among the 11 VIs calculated (NDVI, BNDVI, GNDVI, SAVI, OSAVI, MSAVI, ARVI, CI, TVI, MTVI2, MCARI1), 4 of which have been selected by visual inspection as they better characterize the distinctive components of the imagery such as bare soil, canopy and shadow. Thus, the most responsive 4 are GNDVI, BNDVI, OSAVI and ARVI, with the following mathematical expressions listed below:

Green Normalized Vegetation Index [6]

$$GNDVI = \frac{NIR-GREEN}{NIR+GREEN} \quad (1)$$

Blue Normalized Vegetation Index [7]

$$BNDVI = \frac{NIR-BLUE}{NIR+BLUE} \quad (2)$$

Atmospherically Resistant Vegetation Index, γ=1 [8]

$$ARVI = \frac{NIR-(2*RED)+BLUE}{NIR+(2*RED)-BLUE} \quad (3)$$

Optimized Soil Adjusted Vegetation Index [9]

$$OSAVI = \frac{(NIR-RED)*(1+0.16)}{NIR+RED+0.16} \quad (4)$$

According to the different VIs, threshold values (Table 2) were determined empirically in order to detect "anomalies" linked to XF effects. The limit values were set taking as a reference AOI01 (Fasano), the healthy olive grove, and, subsequently, AOI04 (San Pietro Vernotico), the affected area, was used for verification.

It should be noted that neither of the AOIs was tested through laboratory analyses, however, they were taken as references for the reasons listed below:

- In the AOI01 (Fasano), no dried branch was identified and the harvest has not been subject to negative variations in the last few years. Thus, it can be certainly considered as healthy;
- In the AOI04 (San Pietro Vernotico), that identified among the "affected zones" by the Apulia Region, the trees were almost completely dried. The period of reference and the location of the area (in the proximity of Lecce province) immediately imply the XF presence. Therefore, it can be considered as affected by XF.

TABLE 2. POTENTIALLY HEALTHY RANGE

Threshold Values – Potentially healthy tree	
GNDVI (1)	0.65 - 1.00
BNDVI (2)	0.75 - 1.00
ARVI (3)	0.50 - 1.00
OSAVI (4)	0.25 - 1.00



(a) (b) (c)

Fig. 2. Nadiral acquisition of an olive tree of AOI04, 15 meters AGL: GNDVI (1) vs OSAVI (4) output. The red part of the canopy corresponds to GNDVI values>0.65 (Fig. 2.a), the yellow part of the canopy corresponds to OSAVI values>0.25 (Fig. 2.b).



(a) (b) (c)

Fig. 3. Frontal acquisition of an olive tree of AOI04, 15 meters AGL: GNDVI (1) vs OSAVI (4) output. The red part of the canopy corresponds to GNDVI values>0.65 (Fig. 3.a), the yellow part of the canopy corresponds to OSAVI values>0.25 (Fig. 3.b).

Authorized licensed use limited to: Politecnico di Torino. Downloaded on January 18,2024 at 18:24:35 UTC from IEEE Xplore. Restrictions apply.

V. RESULTS

Analysing the acquisition over the AOI04, it results that OSAVI index produced less alarming results and, above all, incorrect in some cases, since it does not identify correctly the dry branches. Moreover, it was not helpful in identifying any non-symptomatic infected trees. Moreover, the set threshold value (>0.25) did not allow to classify in an appropriate way even the parts that already show evident desiccation. If GNDVI (1), BNDVI (2) or ARVI (3) outputs are taken into account, the dry branches appeared to be correctly classified as "sick" (and therefore not coloured); while the same dry branches were classified as "healthy" (and therefore coloured) based on OSAVI (4) outputs. The inconsistency between GNDVI (Fig. 2.a, Fig.2.b) and OSAVI outputs (Fig. 3.a, Fig. 3.b) was highlighted by circles on an acquisition at canopy scale of the AOI04. The results obtained for AOI04, with respect to OSAVI index (4), were confirmed also for AOI02 and AOI03, where the olive trees do not present any evident signs of the infection. Therefore, the OSAVI index is not suitable for monitoring and prevention purposes, that is the ultimate aim of this work.

In AOI02 and AOI03, some trees present an “anomaly” in the canopy, an “hole”, where the value of the indices was lower than the threshold set (Table 2). The anomalies were clearly visible in the grayscale visualization: the canopy of potentially healthy olive tree appeared to have a homogeneous colour (Fig. 4.b, Fig. 4.c), while the foliage of a potentially affected tree presented some discontinuities (Fig. 5.b, Fig. 5.c), some holes, that are darker with respect to the entire canopy.

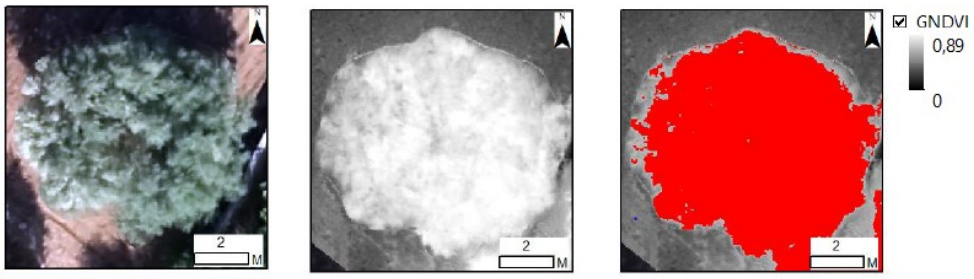
The olive trees identified as anomalous had hardly any dry branches (on the foliage); therefore, the portion of the crown potentially “diseased” associated to a subthreshold value does not mean exclusively dry branches, but also includes green and apparently healthy branches. The true colour visualisation images (Fig. 4.a, Fig. 5.a) show clearly that there is no difference between an healthy canopy and an affected one in the early stage of the disease.

Very concrete feedback regarding these evaluations was received via the results of the laboratory analyses, published on the official Apulian Region Site[1] [1], concerning the XF emergency on 4th November 2021. The trees, considered as "anomalous", since they showed discontinuities in the canopy tested as positive to the presence of the XF bacterium (Fig. 5).

Lastly, as final check to verify the appropriateness of the values ranges used for the analysis of UAV acquisitions, 4 olive trees were considered per area (AOI01, AOI02, AOI03, AOI04).

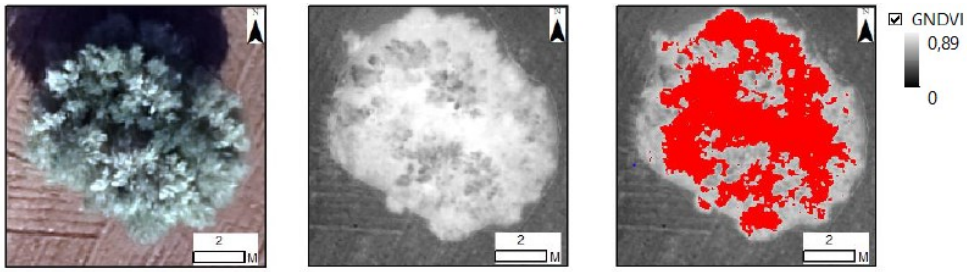
Ten sampling points per tree were selected based on the following considerations:

- For AOI01: all 10 points fall within the portion of healthy canopy;
- For AOI02, AOI03, AOI04: both (potentially) healthy olive trees and (potentially) sick olive trees were considered. For healthy olive trees, all the selected points fall within the lighter portion of the foliage (in the grayscale visualization), while for the potentially affected olive trees, 5 points were taken in the lighter portion and 5 points in correspondence of the "holes" (darker portions in the grayscale visualization).



(a) (b) (c)

Fig. 4. Example of an healthy olive tree (AOI02). Fig 4.a. True colour visualisation . Fig 4.b. GNDVI (1) output - gray scale visualisation. Fig. 4.c. GNDVI (1) output - the red part of the canopy corresponds to GNDVI values>0.65.



(a) (b) (c)

Fig. 5. Example of an affected olive tree (AOI02). Fig. 5.a. True colour visualisation Fig. 5.b. GNDVI (1) output - gray scale visualisation. Fig. 5.c. GNDVI (1) output - the red part of the canopy corresponds to GNDVI values>0.65.gray scale visualisation.

[1] Consultazione Dati Zone Monitoraggio - Fenomeno Xylella Fastidiosa (sit.puglia.it)

Authorized licensed use limited to: Politecnico di Torino. Downloaded on January 18,2024 at 18:24:35 UTC from IEEE Xplore. Restrictions apply.

The mean (Tab. 3) and the median of the values obtained for both "lighter" (green values, in Tab. 3) and "darker" (red values, in Tab. 3) portion are calculated. Based on the values obtained, the following considerations can be inferred:

- For all the AOIs, the values linked to the potentially healthy portion of the canopy were consistent with each other and with the threshold value set. Regardless of the general state of the plant and the presence or absence of a possible infection, a value above the threshold (around the average values identified) indicates a potential healthy portion of the foliage;
- For AOI04, the values in red are related to the desiccation visible to the naked eye, while for the cases of AOI02 and AOI03, the values in red were detected in correspondence of the "holes", thus, they are not linked to dry branches. The values referred are consistent with each VI (with the exception of OSAVI). Regardless of the visibility of desiccation, a subthreshold value (around the average values identified) is an indication of a possible infection/stress of the plant, potentially related to XF.
- The threshold value of the OSAVI index, calibrated on AOI01 and validated on AOI04, was found to be unsuitable for the analyses carried out on AOI02 and AOI03. This conclusion is consistent with the results obtained in the course of the present work: the OSAVI index does not correctly discretize between (potential) healthy and (potential) sick segments.

Analysing the output of the UAV surveys and the detailed photos, at canopy scale, it appears that the ARVI index is more conservative than the GNDVI and BNDVI, in terms of reporting anomalies, The portion of "healthy" foliage, above the threshold values, is greater. Therefore, even if it correctly identifies the desiccation, it is more precautionary than the other two. It was considered appropriate to exclude it from the list of VIs calculated so far, taking into account that the present analysis aims to monitor the effects of the infection.

These conclusions lead to affirm the appropriateness of the computational analyses carried out on the basis of the GNDVI and BNDVI indices, in which the band of near infrared (NIR) is normalized with respect to green (1) and blue (2) band.

A further confirmation of the results achieved was given by one of the most recent studies [10] published on the subject. The research aimed to identify what the best parameters are in the identification of the bacterium in the pre-symptomatic stage.

In terms of VIs, it was observed that the regions of the electromagnetic spectrum most susceptible to XF infection are precisely the bands of blue and green. In particular, the VIs that gave significant results were the NPQI index (Normalized Phaeophytinization Index), linked to the degradation of chlorophyll-pheophytin, and the PRI index (Photechemical Reflectance Index), sensitive to changes in the xanthophyll pigment cycle.

VI. CONCLUSIONS AND FUTURE DEVELOPMENTS

The purpose of the work was to create a sort of workflow aiming to the identify the anomalies on non-symptomatic olive trees, attributable to XF.

The analysis was performed based on the calculation of VIs. Among all, only two of them (GNDVI, BNDVI) provided consistent outputs with each other and corresponding to the tree state of health detected. On the basis of the aforementioned VIs, according to the threshold values (Tab. 2), it was possible to identify some "anomalies" on trees that did not show a visible symptomatology.

The used approach was supported by two important feedbacks received:

- The report of the laboratory analyses, available for AOI02, confirmed the results achieved with the computational analyses. The identified anomalies are potentially related to XF effects.
- In the mathematical expression of GNDVI and BNDVI, NIR band is normalized, with green and blue bands, respectively. A recent study has demonstrated that the regions of the electromagnetic spectrum most susceptible to XF infection are precisely blue and green bands.

Therefore, taking into account the computational analysis, the results achieved and the findings obtained; by the use of multispectral sensors for monitoring the effects of the disease from the pre-symptomatic/initial stage; the validity of the computational approach through the calculation of the Vegetational Indices, GNDVI (1) and BNDVI (2) was confirmed.

TABLE 3. VI MEAN VALUES OF SAMPLING POINTS

VI	Threshold	AOI01		AOI02		AOI03		AOI04	
GNDVI (1)	**0.65**	0.77	-	0.74	0.52	0.69	0.51	0.76	0.55
BNDVI (2)	**0.75**	0.87	-	0.85	0.71	0.82	0.68	0.85	0.70
ARVI (3)	**0.50**	0.78	-	0.73	0.41	0.69	0.43	0.77	0.43
OSAVI (4)	**0.25**	0.46	-	0.57	**0.41**	0.40	**0.40**	0.51	0.21

Authorized licensed use limited to: Politecnico di Torino. Downloaded on January 18,2024 at 18:24:35 UTC from IEEE Xplore. Restrictions apply.

As further developments, the method could be validated on a larger scale in terms of time. Multitemporal surveys would be useful to monitor the XF effects and it could be done by implementing a segmentation algorithm according to the VIs threshold values. The application of the defined algorithm would make the investigation quicker and would make the remote sensing a certificate instrument, as well as the laboratory analyses, for the investigation of the XF.

In addition to this, to integrate, support and strengthen what has been done, taking into account the state of the art and the existent projects (concluded, in progress and being defined), another possible development could be the use of hyperspectral sensors. Such instruments have a higher spectral resolution than that of a multispectral sensor, being able to acquire more than one hundred bands of electromagnetic radiation at a time. The results provided will be more refined, despite a more complex processing in terms higher financial needs (due to the necessary instrumentation) and of working time (due to the amount of data collected).

Since, there is no certified therapy against XF, it is necessary and appropriate that the entire community focuses on acquisitions with UAVs equipped with different sensors in the near future. For the time being, it results the unique way to allow monitoring the progress of the infection in the absence of a pertinent cure.

REFERENCES

[1] K. Scheider, W. van der Werf, M. Cendoya, M. Mourits, J.A.Navas-Cortes, A. Vicent, A.O. Lansink. “Impact of Xylella Fastidiosa subsecies pauca in European Olives”, 2020.

[2] P. J. Zarco-Tejada, C. Camino, P. S. A. Beck, R. Calderon, A. Horner, R. Hernández-Clemente, T. Kattenborn, M. Montes-Borrego, L. Susca, M. Morelli, V. Gonzalez-Dugo, P. R. J. North, B. B. Landa, D. Boscia, M. Saponari, J. A Navas-Cortes. “Previsual symptoms of Xylella fastidiosa infection revealed in spectral plant-trait alterations”, Nature Plants, 4, 432–439, 2018.

[3] Technical Specifications UAV system: P4 Multispectral - Caratteristiche tecniche - DJI

[4] M. Reyniers, D.I. Walvoort, J. De Baardemaaker. (2006). “A linear model to predict with a multi-spectral radiometer the amount of nitrogen in winter wheat”, International Journal of Remote Sensing, 27(19), 4159-4179, 2006.

[5] R.S.Ngamabou. “Evaluating the efficacy of remote sensing techniques in monitoring forest cover and forest cover change in the mount cameroon region” , 2006 (Doctoral dissertation, Verlag nicht ermittelbar).

[6] A.A. Gitelson, Y.J. Kaufman, M.N. Merzlyak, “Use of a Green Channel in Remote Sensing of Global Vegetation from EOS-MODIS”. Remote Sensing of Environment, 58, 1996.

[7] J. Galvan Fraile, J.J. Ramasco, M.A. Matias. “Machine Learning for Remote Sensing of Xylella Fastidiosa”, 2020

[8] Y. J. Kaufman, D. Tanre. "Atmospherically resistant vegetation index (ARVI) for EOS-MODIS". IEEE Transactions on Geoscience and Remote Sensing, 30, pp. 261-270, 1992.

[9] G. Rondeaux, M. Steven, F. Baret. “Optimization of soil-adjusted vegetation indices”. Remote Sensing of Environment, 55, 1996.

[10] P. J. Zarco-Tejada, T. Poblete, C. Camino, V. Gonzalez-Dugo, R. Calderon, A. Hornero, R. Hernandez-Clemente, M. Romàn-Ecija, M. P. Velasco-Amo, B. B. Landa, P. S. Beck, M. Saponari, D. Boscia, J. A. Navas-Cortes. “Divergent abiotic spectral pathways unravel pathogen stress signals across species”, Nature Communications, 12(1), 1-11, 2021.

[11] S. De Petris, P. Boccardo, E. Borgogno Mondino. “Detection and characterization of oil palm plantations through MODIS EVI time series”, International Journal of Remote Sensing, 40(19), 7297-7311, 2019.

[12] T. Bellone, P. Boccardo, F. Perez. “Investigation of Vegetation Dynamics using Long-Term Normalized Difference Index Time-Series”, American Journal of Environmental Sciences, 5(4), 461, 2009.

Authorized licensed use limited to: Politecnico di Torino. Downloaded on January 18,2024 at 18:24:35 UTC from IEEE Xplore. Restrictions apply.